nature sustainability

Article

https://doi.org/10.1038/s41893-025-01616-7

Heavy metal imprints in Antarctic snow from research and tourism

Received: 24 February 2025

Accepted: 17 July 2025

Published online: 20 August 2025

Check for updates

Raúl R. Cordero[1,2], Sarah Feron[1] ✉, Avni Malhotra[3], Alessandro Damiani[4], Minghu Ding[5], Francisco Fernandoy[6], Juan A. Alfonso[7], Belkis Garcia[7], Juan M. Carrera[7], Pedro Llanillo[8], Paul Wachter[9], Jaime Pizarro[2] ✉, Elise Roumeas[1], Edgardo Sepúlveda[10], Jose Jorquera[2], Chenghao Wang[11,12], Jorge Carrasco[13], Zutao Ouyang[14], Pedro Oyola[15], Maarten Loonen[1], Anne Beaulieu[1], Jacob Dana[16], Alia L. Khan[16,17], Gino Casassa[13,18] & Choong-Min Kang[19]

Antarctica, long regarded as one of the last pristine environments on Earth, is increasingly affected by human activity. As tourism surges and scientific operations expand, air pollution from local emissions is raising new environmental concerns. Here we analyse surface snow samples collected along a ~2,000-km transect, from the South Shetland Islands (62° S) to the Ellsworth Mountains (79° S), to map the geochemical fingerprints of aerosol deposition. We identify distinct spatial patterns shaped by crustal, marine, biogenic and anthropogenic sources. Notably, we detect heavy metal imprints in the snow chemistry of the northern Antarctic Peninsula, where major research stations are concentrated and marine tourism traffic is most intense. Our findings shed light on the extent of the impacts from energy-intensive local activities in Antarctica, underscoring the need for enhanced environmental monitoring and sustainable management strategies in this fragile region.

The Antarctic continent, often perceived as a pristine wilderness, is increasingly under environmental pressure from growing human activities (Fig. 1). This pressure is particularly intense in the Antarctic Peninsula, the fastest-warming region on the continent[1] and the busiest area for marine traffic[2] (Fig. 1a,b). According to data from the International Association of Antarctica Tour Operators (IAATO)[3], over 120,000 visitors travelled with IAATO members to the region during the 2023–2024 season, most of them aboard a fleet of 93 vessels (Fig. 1c). The Antarctic Peninsula also hosts about half of the research facilities on the continent (Supplementary Fig. 1). Data from the Council of Managers of National Antarctic Programs[4] indicate that 114 research facilities are actively in use within the Antarctic Treaty area, with a combined accommodation capacity of over 5,000 beds for scientists and staff (Fig. 1d).

While essential for science and global outreach, the increasing human presence in Antarctica raises concerns about pollutants from fossil fuel combustion, including those from ships, aircraft, vehicles and supporting infrastructure (for example, refs. 5–8). Fuel combustion emissions vary with engine type, load and fuel specifications but

[1]University of Groningen, Leeuwarden, the Netherlands. [2]Universidad de Santiago de Chile, Santiago, Chile. [3]Biological Sciences Division, Pacific Northwest National Laboratory, Richland, WA, USA. [4]Center for Climate Change Adaptation, National Institute for Environmental Studies, Tsukuba-shi, Japan. [5]State Key Laboratory of Severe Weather, Chinese Academy of Meteorological Sciences, Beijing, China. [6]Universidad Andrés Bello, Viña del Mar, Chile. [7]Instituto Venezolano de Investigaciones Cientificas, Caracas, Venezuela. [8]Centro Oceanográfico de Canarias, Instituto Español de Oceanografía, Santa Cruz de Tenerife, Spain. [9]German Aerospace Center, German Remote Sensing Data Center, Wessling, Germany. [10]Department of Chemical and Environmental Engineering, University of Arizona, Tucson, AZ, USA. [11]School of Meteorology, University of Oklahoma, Norman, OK, USA. [12]Department of Geography and Environmental Sustainability, University of Oklahoma, Norman, OK, USA. [13]University of Magallanes, Punta Arenas, Chile. [14]College of Forestry, Wildlife and Environment, Auburn University, Auburn, AL, USA. [15]Centro Mario Molina, Santiago, Chile. [16]Western Washington University, Bellingham, WA, USA. [17]National Snow and Ice Data Center, Cooperative Institute for Research in Environmental Sciences, University of Colorado, Boulder, Boulder, CO, USA. [18]Instituto Antártico Chileno, Punta Arenas, Chile. [19]Harvard School of Public Health, Boston, MA, USA. ✉e-mail: s.c.feron@rug.nl; jaime.pizarro@usach.cl

https://doi.org/10.1038/s41893-025-01616-7

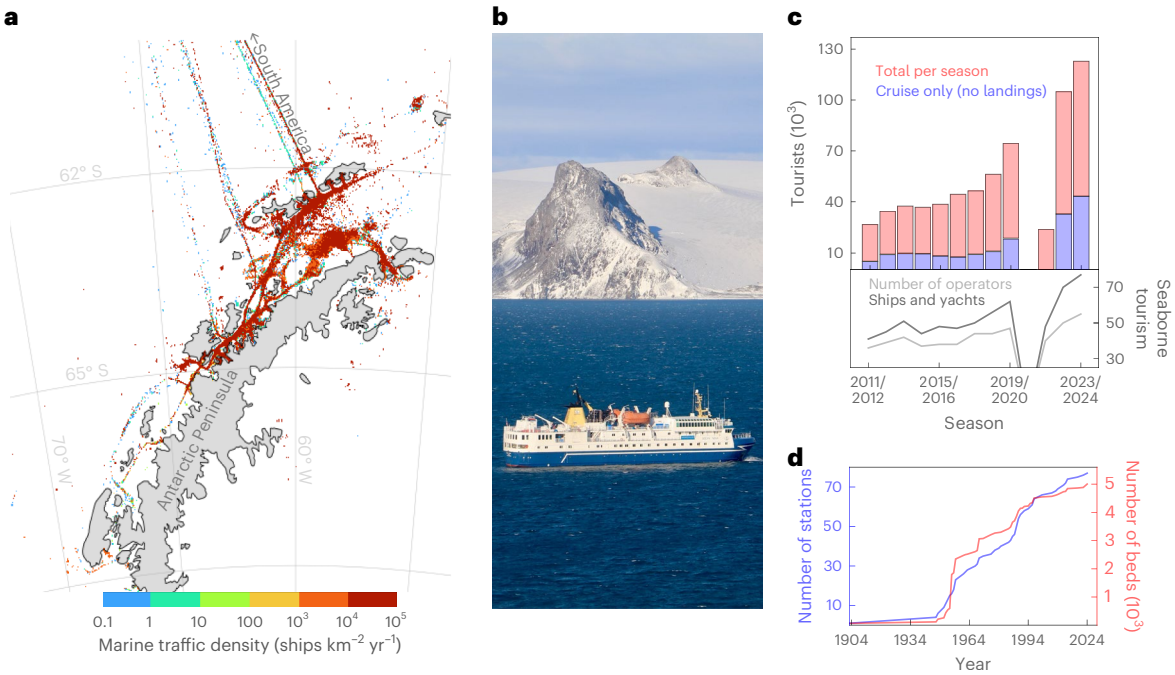

Fig. 1 | Antarctic tourism quickly rebounded after the SARS-CoV-2 pandemic. **a**, A density map of marine traffic over the period January 2015 to February 2021. Most visitors travelling to Antarctica with the IAATO embark on ships to cruise the Antarctic Peninsula. According to data from IMF's World Seaborne Trade monitoring system[60], marine traffic is considerably more intense around the northern Antarctic Peninsula. **b**, A tourist vessel in Maxwell Bay, King George Island. IAATO now includes over 50 operators, with a fleet of 93 vessels (including 9 large cruise ships) that collectively registered 569 departures during the 2023–2024 season[3]. In addition, 787 visitors engaged in deep-field and air-based Antarctic tourism during the same season, with about half of them staying at Union Glacier Camp[70]. **c**, The number of tourists, IAATO operators and IAATO vessels from the 2011–2012 season onwards. The number of tourists visiting Antarctica has quadrupled over the past decade. Approximately a quarter of Antarctic tourists travel on cruise-only vessels (that is, carrying more than 500 passengers). **d**, The number of research facilities from 1903 onwards. There are currently 114 research facilities in Antarctica (including seasonal facilities)[4]. Approximately half of these research facilities are located in the Antarctic Peninsula[4]. Plots were generated using Python's Matplotlib library (version 3.4.3)[71]. Photograph taken by the authors.

are known to include particles containing metalloid and metal elements such as Cr, Ni, Cu, Zn and Pb (ref. 9). In vulnerable ecosystems, the accumulation of heavy metals poses risks to microbial communities, primary producers and higher trophic levels through bioaccumulation and potential biomagnification[10–12]. The contamination of soil and marine environments near older Antarctic research stations has been well documented (for example, refs. 13–15). However, due to sparse ground-based atmospheric measurements (for example, refs. 16,17), air pollution from local sources in Antarctica remains poorly studied.

Antarctic snow chemistry offers valuable insights into the impact of human activities on the continent[18]. Snow has the unique property of collecting atmospheric aerosols, making its composition a direct indicator of air quality[19–22]. Long-range atmospheric transport plays a role in delivering trace elements to the continent's vast interior, far from any local sources. For example, dust from South America[23] and anthropogenically enriched particulate matter from Australia[24] have been found in Antarctic snow and ice. However, the strong westerly winds that encircle Antarctica limit meridional airborne transport[25,26], keeping background levels of these elements very low (on the order of parts per trillion or picograms per gram)[27–31]. By contrast, snow samples collected near research facilities often exhibit heavy metal concentrations several orders of magnitude higher[32–35], highlighting the environmental impact of energy-intensive research activities. Less attention has been given to the environmental effects of the tourist industry.

The focus of prior research on the contamination footprint (as defined by Brooks et al.[36]), primarily around heavily impacted sites in the immediate vicinity of research facilities, has left a gap in understanding the broader spatial patterns of environmentally consequential trace metals across Antarctica. To address this gap, we conducted an extensive survey of Antarctic snow at 16 sites (Fig. 2a and Table 1) along a transect of approximately 2,000 km, encompassing all major Antarctic tourist hotspots. The majority of sampling sites were located on the Antarctic Peninsula and surrounding archipelagos, broadly reflecting typical tourist routes. Most cruises visit the South Shetland Islands and the Palmer Archipelago, as well as smaller islands off the Antarctic Peninsula such as Cuverville (64° S), Petermann (65° S) and Detaille (67° S). Our southernmost sampling site was the Ellsworth Mountains (79° S), which have also become a popular tourism destination.

Using X-ray fluorescence (XRF) spectrometry, we measured the elemental concentrations of insoluble particles (>0.4 µm) in 55 surface snow samples (0–20 cm depth) collected over four consecutive summer seasons (2016–2017 to 2019–2020). To assess the influence of local sources on representative areas, we deliberately avoided sampling at sites near legacy pollutants[37]. Instead, sampling sites were strategically selected to be hundreds of metres (and, whenever possible, several kilometres) away from obvious aerosol sources such as research stations, tourist shore landing sites, roads, airfields, penguin colonies and wildlife nesting areas. Our measurements allowed us to test the hypothesis that the footprint of energy-intensive local activities extends beyond heavily impacted sites near century-old research facilities.

Results

Geographical patterns

XRF spectrometry was used to measure the concentrations of 48 elements, with only 27 found to be above the detection limits (Supplementary Table 1). Principal component (PC) analysis (PCA) applied to these measurements revealed distinct geographical patterns and the interplay of crustal, marine, biogenic and anthropogenic contributions

https://doi.org/10.1038/s41893-025-01616-7

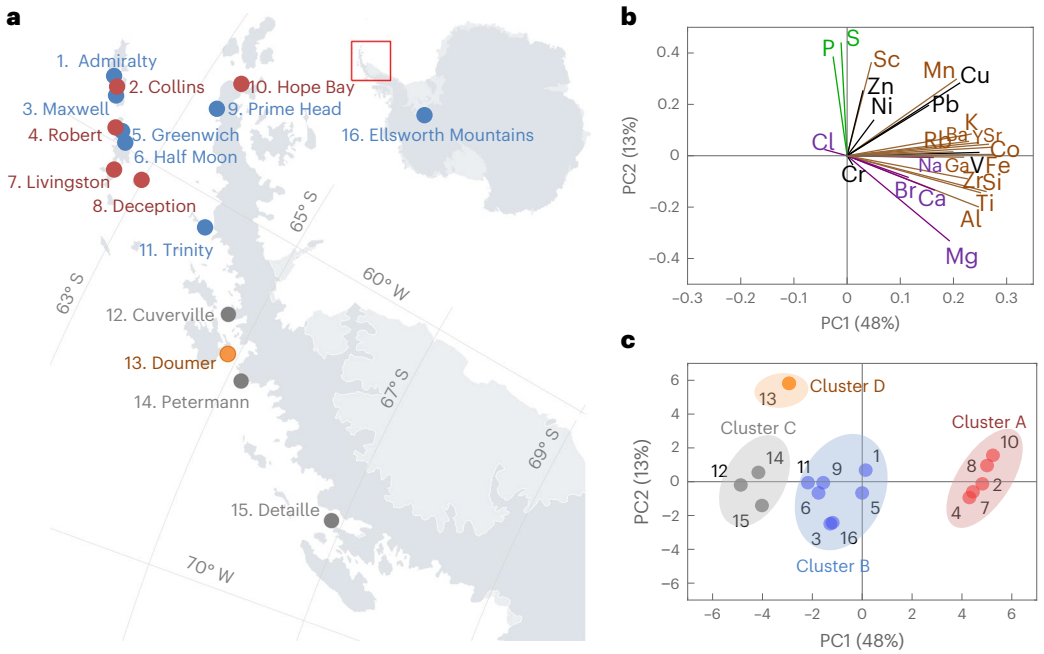

Fig. 2 | Snow chemistry across our sampling sites exhibit both natural and anthropogenic markers. a, Snow sampling sites. Colours represent the clusters identified by applying PCA to the element concentrations in Supplementary Table 1. Sampling was conducted at 16 sites, marked by consecutive numbers. We sampled across the South Shetland Islands (King George Island, Robert Island, Greenwich Island, Half Moon Island, Livingston Island and Deception Island) and the Palmer Archipelago (Trinity Island and Doumer Island), along or near the west coast of the Peninsula (Prime Head, Hope Bay, Charlotte Bay, Cuverville Island, Petermann Island and Detaille Island) and at deep-field points in the Ellsworth Mountains (Union Glacier). Refer to Table 1 for details. **b**, PC loadings showing contributions to the first two PCs (PC1 and PC2). The loadings are also provided in Supplementary Table 2. PC1 and PC2 explain 61% of the total variance. Colours represent likely sources: purple for elements typically associated with marine aerosols, brown for crustal sources, green for possible biogenic or non-sea-salt contributions and black for potential anthropogenic markers. **c**, PC scores. Points close to each other represent sampling sites with similar elemental profiles. The distribution suggests 4 potential clusters among the 16 sampling sites (identified by consecutive numbers). The first two PCs (PC1 and PC2) explained about 61% of the total variance and were influenced by elements associated with marine aerosols, crustal sources, biogenic and non-sea-salt contributions, and potential anthropogenic markers. Colours for the sites match those in **a**. The plot in **a** was created using Python's Matplotlib library (version 3.4.3)[71], while plots in **b** and **c** were generated using Mathematica version 12 (ref. 54).

to Antarctic snow chemistry (Fig. 2, Supplementary Fig. 2 and Supplementary Tables 2–5). The first two PCs (PC1 and PC2) explained about 61% of the total variance and were influenced by elements associated with marine aerosols (for example, Na, Mg and Ca), crustal sources (for example, Al, Si, Fe, Ti, Y and Zr), biogenic and non-sea-salt contributions (for example, P and S) and potential anthropogenic markers (for example, Ni, Pb, Cu, Cr and Zn).

The contributions of crustal dust and sea salt were coupled across the study area. The PC loadings plot (Fig. 2b) suggests a positive correlation between elements associated with marine aerosols (for example, Na and Mg) and crustal sources (for example, Al, Si, Fe, Ti, Y and Zr). These elements strongly contributed to PC1, reflecting its association with sea salt aerosols and dust inputs. The coupling between crustal dust and sea salt is not surprising, as both are wind-driven aerosols.

The concentration of anthropogenic markers showed little to no correlation with natural aerosols, such as crustal dust or sea-salt particles. The PC loadings plot (Fig. 2b) highlights that anthropogenic markers (for example, Ni, Pb, Cu, Cr and Zn) and elements associated with biological or secondary processes (for example, P and S) exhibited weak or negligible correlations with marine salts (for example, Na and Mg) and crustal elements (for example, Al, Si, Fe, Ti, Y and Zr). The strong contribution of metals commonly linked to fossil fuel pollution (for example, Ni, Pb, Cu, Cr and Zn) to PC2 underscores its association with anthropogenic inputs. The decoupling of anthropogenic markers from crustal dust and sea-salt particles suggests that PC2 is influenced by local sources (related to marine traffic and research facilities).

Elemental concentrations across the study area exhibited distinct elemental profiles, suggesting four clusters among the sampling sites (Fig. 2c and Supplementary Fig. 3). PC1 separates the data into three clusters (A, B and C), reflecting differences in the concentrations of sea salt aerosols and crustal dust. As shown in Fig. 3a and Supplementary Table 5, concentrations of elements associated with marine aerosols (for example, Na and Mg) and crustal sources (for example, Al, Si, Fe, Ti, Y and Zr) differed considerably across these clusters, with cluster A showing the highest concentrations, followed by clusters B and C. PC2 identifies a fourth cluster (D), characterized by prominent biogenic and non-sea-salt contributions. Samples taken in Doumer Island (cluster D) exhibited concentrations of P (an element associated with biogenic and non-sea-salt inputs) one order of magnitude higher than those in clusters A, B and C (Fig. 3a and Supplementary Table 5).

While concentrations of anthropogenic markers were generally comparable (within the same order of magnitude) across the identified clusters (Fig. 3a), we found north–south differences in metal concentrations consistent with expectations. As shown in Supplementary Table 5, the concentrations of elements associated with fossil fuel combustion (for example, Ni, Pb, Cu, Cr and Zn) were slightly higher in the northernmost sites (clusters A and B) compared with the southernmost sites (cluster C). Correspondingly, Supplementary Table 1 shows that the highest heavy metal concentrations were found at northern locations such as Admiralty Bay (site 1) and Hope Bay (site 10), both situated near major research stations and along busy marine routes.

Natural contributions

Crustal dust dominates the loadings across the sampling sites. Ti/Zr ratios of 18–40, observed for each of the four clusters (Fig. 3b and Supplementary Table 6), indicate a crustal or natural mineral dust

https://doi.org/10.1038/s41893-025-01616-7

Table 1 | Sampling sites

Site	Point	Latitude (°)	Longitude (°)	Season	Details
(1) Admiralty Bay	Arctowski Station	−62.1203	−58.6453	19/20	Our fieldwork on King George Island encompassed several sampling points on Collins Glacier (that blankets roughly 75% of the island) as well as two of its three principal bays: Maxwell Bay and Admiralty Bay. King George Island is the largest in the South Shetland archipelago and hosts research stations from nine countries and one of Antarctica's most active airfields. During the 2023–2024 season, around 5% of all visitors travelling with IAATO-affiliated operators to Antarctica used King George Island as a flight hub, often combining air travel with cruises.
(2) Collins Glacier	Collins A	−62.1673	−58.8547	17/18	
	Dome	−62.1686	−58.8753	19/20	
	Collins B	−62.1698	−58.8586	16/17	
	Collins C	−62.1691	−58.8555	19/20	
	Artigas Station	−62.1833	−58.8844	19/20	
(3) Maxwell Bay	Escudero Station	−62.2028	−58.9608	16/17	
	Ardley	−62.2167	−58.9333	16/17	
	Great Wall Station	−62.2238	−58.9635	17/18	
(4) Robert Island	Coppermine Peninsula	−62.3786	−59.7119	16/17	We conducted our sampling on the island's west side, an area characterized by a variety of terrestrial fauna and a rich bird population. The island also hosts a seasonally occupied research refuge.
(5) Greenwich Island	Prat Station	−62.4798	−59.6434	19/20	This island hosts large penguin colonies and is also the site of two research stations. Sampling was carried out approximately 1 km west of one of these stations.
(6) Half Moon	Half Moon Bay	−62.5956	−59.9122	18/19	This small island is a popular stop on Antarctic cruise routes, home to Weddell and elephant seals, as well as penguin colonies. It also features an Argentine station that operates intermittently.
(7) Livingston Island	Walker Bay A	−62.6364	−60.6008	19/20	Sampling was carried out near Hannah Point, a well-known tourist landing site renowned for its rich biodiversity, including some of the most diverse wildlife in the Antarctic Peninsula. The island is also home to research stations. At its western edge lies Byers Peninsula, a sizable ice-free area spanning 6,062 ha, which serves as a potential source of dust.
	Walker Bay B	−62.6362	−60.6010	19/20	
(8) Deception Island	Mount Pond	−62.9656	−60.5522	19/20	This horseshoe-shaped island is a well-known tourist destination and is home to research stations operated by Argentina and Spain. During the summer, much of the island becomes ice-free. Sampling took place along the southwestern coast and near the Spanish research station.
	G. de Castilla Station	−62.9768	−60.6691	18/19	
(9) Prime Head	O'Higgins Station	−63.3225	−57.8970	18/19	Sampling took place near the permanently occupied Chilean research station, situated close to the northernmost tip of the peninsula.
(10) Hope Bay	Esperanza Station	−63.4078	−56.9911	19/20	Sampling took place a few kilometres from a major year-round Argentinian station that has been operational since the early 1950s.
(11) Trinity Island	Mikkelsen Harbor A	−63.8967	−60.8025	18/19	Sampling took place near the southernmost point of the island, a popular landing site for cruise tourists visiting Antarctica. The island is also home to a small refuge, originally established by the Argentine Navy in the 1950s.
	Mikkelsen Harbor B	−63.9133	−60.8150	19/20	
(12) Cuverville Island	Northern Shore	−64.6803	−62.6194	16/17	Sampling was conducted along the northern coastline of the Island, which is known for its historic remains (from the whaling era) and penguin colonies.
(13) Doumer Island	Yelcho Station A	−64.8761	−63.5783	19/20	Sampling was conducted near the local research station. Marine wildlife around the island includes seals, penguins and seabirds. Major algal fields are often frequent.
	Yelcho Station B	−64.8775	−63.5831	19/20	
	Yelcho Station C	−64.8779	−63.5824	19/20	
(14) Petermann Island	Groussac Refuge	−65.1758	−64.1361	18/19	This small island is a popular stop for Antarctic cruises due to its scenic views and wildlife, which includes large colonies of gentoo penguins.
(15) Detaille Island	Station W	−66.8687	−66.7833	16/17	We collected samples near the unoccupied UK station established in the 1950s. The site is visited by small expedition cruise ships.
(16) Ellsworth Mountains	Union Glacier A	−79.7669	−82.9144	16/17	This area features a blue-ice runway and two seasonal camps that provide expedition logistics and guided tours. Sampling was conducted at two points situated more than 5 km east of a blue-ice runway and less than 1 km from designated landing areas for ski-equipped aircraft.
	Union Glacier B	−79.7625	−82.9603	18/19	

In some cases, a sampling site encompassed several sampling points, spaced a few hundred metres apart.

origin, with contributions from slightly weathered rocks and minimal chemical fractionation. K/Rb ratios of 200–600, observed across our sampling sites (Fig. 3b and Supplementary Table 6), are also consistent with values found in continental crust and terrestrial dust. Moderate Si/Al and Si/Ti ratios (Fig. 3b and Supplementary Table 6) further confirm the influence of terrestrial dust and crustal material, as well as moderate weathering processes. Comparable Si/Al ratios (within the same order of magnitude) have also been reported in samples

https://doi.org/10.1038/s41893-025-01616-7

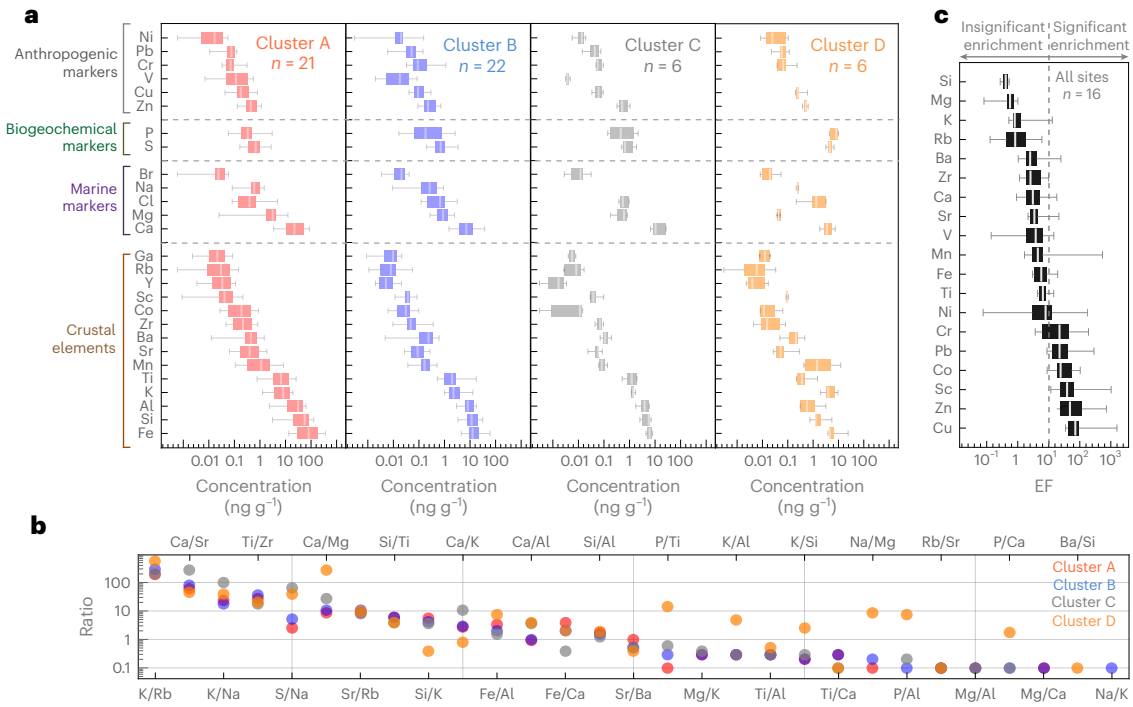

Fig. 3 | Metal concentrations at the sampling sites exceeded the background levels. a, Box plots showing the concentrations in snow samples, grouped by clusters (*n* indicates the number of samples per cluster). In each box plot, the central line represents the median, while the edges of the box indicate the 25th and 75th percentiles. Whiskers extend to the minimum and maximum values, excluding outliers. **b**, Geochemical proxies or ratios of element concentrations averaged by cluster. The colours represent different clusters. Ratios are also presented in Supplementary Table 6. **c**, Box plots showing EFs derived from element concentrations in Supplementary Table 1 (*n* indicates the number of sites). In each box plot, the central line represents the median, while the edges of the box indicate the 25th and 75th percentiles. Whiskers extend to the minimum and maximum values, excluding outliers. EF values greater than 10 indicate contributions from anthropogenic sources. EF values for heavy metals commonly associated with fossil fuel pollution, such as Pb, Cu and Zn, were consistently above 10 across all sampling sites. Plots were created using Python's Matplotlib library (version 3.4.3)[71].

from glaciers on James Ross Island in the northeastern Antarctic Peninsula[38]. While long-range transport from Patagonia cannot be ruled out[39], Antarctica itself also contains vast potential dust sources (Supplementary Fig. 4).

Ice-free areas appear to be key sources of dust and crustal material, even for deep-field sites. In the northern Antarctic Peninsula, for example, the Ulu Peninsula covers approximately 312 km^2 and is ice-free during the summer. Similarly, about half of Deception Island (around 17 km^2), the southwestern tip of King George Island (about 30 km^2; Supplementary Fig. 5) and the Byers Peninsula (around 60 km^2), located at the western extremity of Livingston Island, are all notable ice-free regions. The presence of these ice-free areas probably explains why sites in clusters A and B exhibited the highest concentrations of elements associated with crustal sources (for example, Al, Si, Fe, Ti, Y and Zr) (Fig. 3a). Farther south, the ice-free summits of the Ellsworth Mountains (Supplementary Fig. 6) were probably the primary source of dust and crustal material found in the snow samples collected at our southernmost sampling site, Union Glacier (79° S).

Although most sampling sites were coastal, marine salt particulates did not dominate the aerosol loadings. The concentration of Na, a primary marker of sea salt, was generally much lower than the concentrations of elements associated with crustal sources, such as Al, Si, Fe and Ti (Fig. 3a). The relatively low concentration of Na in the insoluble fraction of particulate matter in our samples may be due to its solubility. By contrast, elements such as Al, Si, Fe and Ti are largely insoluble. Due to the relatively low concentration of Na, we found that Na/K and Na/Mg ratios were well below 1 at all sampling sites, except for Doumer Island. Nevertheless, we also found moderate S/Na ratios, which indicate marine aerosol influence. Sulfur in marine aerosols is often present as sulfate particles, which form through the nucleation of sulfur-containing gases or the condensation of these gases onto preexisting particles (for example, ref. 40).

Marine-enriched aerosols (that is, phytoplankton and sea spray) and biogenic sources (that is, penguins, seals and snow organisms) played a considerable role in the chemistry of our samples, especially those taken on Doumer Island (cluster D). The moderate values of Ca/Sr and Ca/K ratios (Fig. 3b and Supplementary Table 6) suggest the presence of marine aerosols with possible biogenic sulfur influences, including those from marine organisms such as phytoplankton, across the sampling sites. Comparable Ca/Sr and Ca/K ratios have also been reported in snow collected elsewhere in the northeastern Antarctic Peninsula[38]. An additional biogenic source, specifically snow algae (Supplementary Fig. 7), probably influenced the elemental composition of samples on Doumer Island. Relative to other clusters, cluster D exhibits a combination of elevated P/Al, P/Ti, K/Si and K/Al ratios (Fig. 3b and Supplementary Table 6), consistent with the influence of snow algae, which could explain the enrichment of P and K relative to typical crustal markers such as Al, Si and Ti. The presence of algal biomass would not be particularly surprising, as algae thrive in coastal areas, which are nutrient-rich environments[41,42].

Anthropogenic markers

The concentrations of anthropogenic markers across our sampling sites significantly exceeded background levels (Supplementary Fig. 8). Background concentrations of heavy metals in snow on the Antarctic Peninsula were established in the 1980s. Wolff and Peel[28] reported average concentrations of approximately 2 pg g^{-1} Cu, 3 pg g^{-1} Zn and 6 pg g^{-1} Pb in surface samples taken on Spaatz Island and the southern Palmer Plateau. Leal et al.[29] reported average concentrations of approximately 10 pg g^{-1} Cr, 3 pg g^{-1} Ni and 10 pg g^{-1} Pb in fresh

snow samples taken nearly two decades ago at Admiralty Bay, King George Island. Comparable Pb concentrations were also measured by Hong et al.[30] about two decades ago at Collins Dome on King George Island. Measurements by Leal et al.[29] and by Hong et al.[30] are relevant because they were conducted well before the recent tourism boom, yet at a time when the island already hosted nearly a dozen research facilities[4]. Relative to these values, we found that Pb, Ni and Cr concentrations across our sampling sites were, on average, tenfold higher, while Cu and Zn concentrations were, on average, two orders of magnitude higher.

Metal concentrations measured across the Antarctic Peninsula were well above those in unimpacted regions of the continent (Supplementary Fig. 8). Dixon et al.[31] provided a baseline of trace element concentrations across extensive regions of Antarctica (excluding the Antarctic Peninsula). For metals, Dixon et al.[31] reported average concentrations of approximately 8 pg g^{-1} Cr, 14 pg g^{-1} Mn, 12 pg g^{-1} Sr and 6 pg g^{-1} Pb in surface samples. Comparable Pb concentrations have been measured in surface snow sampled upwind of the research facilities (clear area) near the South Pole[33], in snow pit samples from unimpacted Roosevelt Island in the Ross Sea region[27], in snow from Dome C sampled over the period 2010–2017[24] and along the transect from Zhongshan Station to Dome A[43]. Relative to these values, we found that Pb, Cr and Sr concentrations across our sampling sites were, on average, tenfold higher, while Mn concentrations were, on average, two orders of magnitude higher.

The application of enrichment factor (EF) analysis to XRF measurements led to moderate EF values (generally above 10) for heavy metals, particularly Pb, Cu and Zn, across our sampling sites (Fig. 3c and Supplementary Table 7). As noted by Veysseyre et al.[44], EF values between 0.1 and 10 suggest that an element primarily originates from natural sources, such as rocks and dust, while EF values greater than 10 indicate contributions from additional sources. While most element concentrations in the snow sampled during our study aligned with average upper-crustal ratios, as shown in Fig. 3c and Supplementary Table 7, the EF values for heavy metals typically linked to fossil fuel pollution (Pb, Cu and Zn) were consistently close or higher than 10 across all sampling sites, including Union Glacier (79° S), our southernmost sampling site. The generator powering at least one of the two seasonally occupied camps, the heavy aircraft utilizing the blue-ice runway and the ski-equipped planes (Supplementary Fig. 6) are likely contributors to the heavy metals detected in the surface snow sampled at this increasingly popular deep-field destination.

Although our sampling sites are polluted, the concentrations of toxic elements such as As, Cd and Se were found to be minor. The average concentrations measured for these elements were well below the detection limit of XRF spectrometry, which is why these concentrations are not shown in Fig. 3 and Supplementary Table 1. Concentrations considerably higher, detectable by XRF spectrometry, have been measured elsewhere in Antarctica. Notably, significant concentrations of Cd have been found in surface snow near the research station at Dome Concordia[32], presumably from anthropogenic sources. Similarly, significant concentrations of Cd and As have been measured in surface snow sampled near research facilities at the South Pole[33]. Furthermore, significant concentrations of Cd, As and Se have been measured in surface snow from Ingrid Christensen Coast, near research stations such as Progress (Russia), Zhongshan (China) and Bharati (India) in East Antarctica[34]. By comparison, the concentrations across our sampling sites were probably several orders of magnitude lower. These differences were expected, as we avoided sampling at heavily impacted sites too close to research stations or areas affected by legacy pollutants.

Surface snow across our sampling sites was generally cleaner than that sampled close to research facilities in the Antarctic Peninsula and elsewhere. Surface snow from the Vecherny Oasis, near the Belarusian Antarctic Station in East Antarctica, reported average concentrations over the summer period of 2012–2018 of approximately 1 ng g^{-1} Cu, 16 ng g^{-1} Zn and 0.2 ng g^{-1} Pb (ref. 35). Average concentrations in surface snow from Ingrid Christensen Coast, near research stations like Progress (Russia), Zhongshan (China) and Bharati (India) in East Antarctica, are similarly high: 2 ng g^{-1} Cu, 5 ng g^{-1} Zn and 0.4 ng g^{-1} Pb (ref. 34). Relative to these figures, we found that Cu, Zn and Pb concentrations across our sampling sites were, on average, one order of magnitude lower. Again, these differences were expected, as we deliberately avoided sampling at heavily impacted sites, targeted by previous studies.

Meridional gradient

Natural aerosols, such as crustal dust and sea-salt particles, decreased in concentration towards the south. While crustal dust dominates the loadings across all sampling sites, the concentrations of elements associated with crustal sources (for example, Al, Si, Fe, Ti and Y) show a significant decline with increasing latitude on the Antarctic Peninsula (Fig. 4a). A similar trend is observed for elements linked to marine aerosols, such as Na, Mg and Ca (Fig. 4a). The decrease in concentrations toward the south of key markers for crustal material (for example, Al, as shown in Fig. 4b, left) was expected, as ice-free areas, presumably the main source of crustal dust, become less prominent further south. Likewise, the reduction in Na concentrations (Fig. 4b, centre) can be attributed to the weakening of surface winds at higher latitudes (Supplementary Fig. 9), which may limit the transport of sea-salt particles. Because our sampling took place in late summer, it is unlikely that sea ice had a relevant influence on the observed spatial distribution of natural aerosols.

In the Antarctic Peninsula, elements associated with biogenic and non-sea-salt sources (for example, P) generally showed higher concentrations at our sampling sites on Doumer Island (~65° S) compared with King George Island (~62° S) (Supplementary Fig. 10). The higher concentrations observed on Doumer Island can probably be attributed to biogenic sources such as snow algae, organisms that grow on snow and ice, produce organic matter and influence the elemental composition through their metabolic activity. Gray et al.[41] mapped algal fields across the Antarctic Peninsula and showed that the number of individual algal blooms increases progressively southward from 62° S, peaking around 65° S, before decreasing further south. This pattern is consistent with changes in environmental conditions favourable to biological activity at these latitudes. Although temperatures are lower at 65° S than at 62° S, the increased availability of sunlight in this region supports algal growth. As shown in Supplementary Fig. 11, a decrease in cloud cover results in higher downwelling shortwave irradiance at Doumer Island (65° S) compared with King George Island (62° S), further enhancing conditions for algal growth.

Heavy metal concentrations (for example, Ni, Pb, Cu, Cr and Zn) do not exhibit a clear meridional (north–south) gradient (Fig. 4a). This is because the concentrations of these potential anthropogenic markers are comparable (within the same order of magnitude) across the identified clusters (Fig. 3a and Supplementary Table 5). The lack of a clear meridional gradient in heavy metal concentrations is consistent with the limited meridional airborne transport and Antarctica's isolation resulting from the stronger westerlies over the Southern Ocean (Supplementary Fig. 9). Back-trajectory analysis, which traces the path of air masses backwards in time to determine their geographical origin, further confirms limited meridional atmospheric transport. As shown in Supplementary Fig. 12, while long-range transport accounts for background concentrations observed inland (for example, ref. 26), it probably plays only a minor role in contributing to the heavy metals detected in our samples (Supplementary Fig. 12).

The absence of a clear meridional gradient in concentrations of anthropogenic markers does not imply that some sites are not considerably more polluted than others. For instance, Pb concentrations at Admiralty Bay (the northernmost sampling site) and Hope Bay (near the northern tip of the Peninsula) are noticeably higher than those at southern Antarctic Peninsula sites, such as Detaille Island (Fig. 4b, right). This pattern aligns with expectations, as marine traffic (a potential source

https://doi.org/10.1038/s41893-025-01616-7

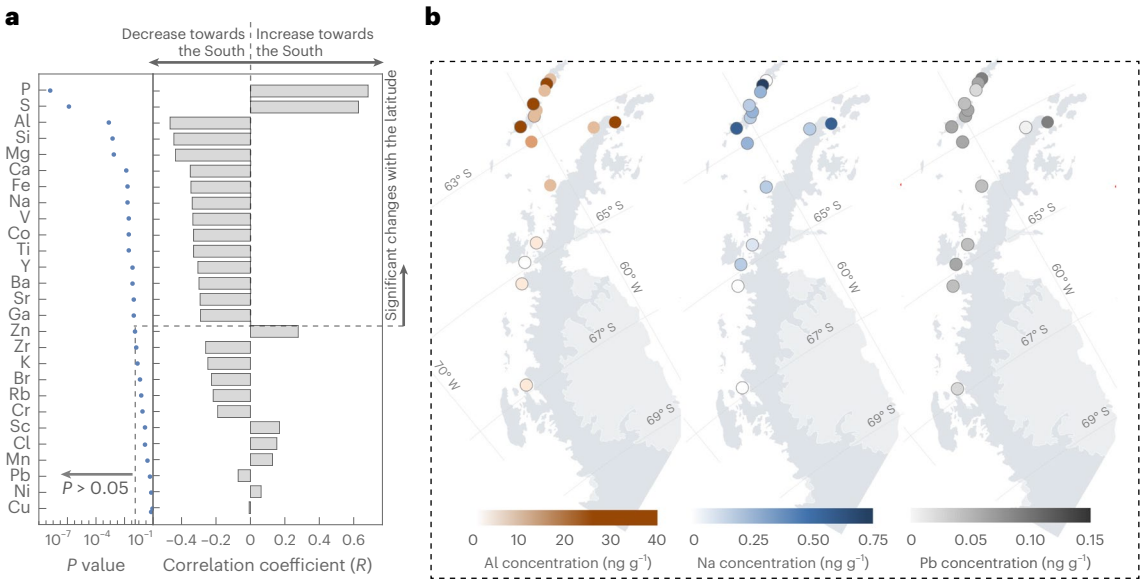

Fig. 4 | In the northern Antarctic Peninsula, the concentrations of more than half of the measured elements vary significantly with latitude. a, Linear regressions between latitude and element concentrations in samples collected across the northern Antarctic Peninsula (sites 1–14): *P* values on the left and two-sided Pearson correlation coefficients (*R*) on the right. Elements are ranked top to bottom based on *P* values. Correlations with *P* values lower than 0.05 are considered significant. **b**, Colour-coded element concentrations (nanograms per gram of snow) in samples collected across the Antarctic Peninsula: Al (left), Na (centre) and Pb (right). Despite the lack of statistically significant meridional gradient, Pb concentrations at Admiralty Bay (the northernmost sampling site) and Hope Bay (near the northern tip of the Peninsula) are clearly higher than those at more southerly sites, such as Detaille Island. Plots were created using Python's Matplotlib library (version 3.4.3)[71].

of heavy metals) is considerably more intense around the northern Antarctic Peninsula (Fig. 1a).

Discussion

Our analysis of Antarctic snow chemistry has revealed distinct geographical patterns shaped by the interplay between crustal, marine, biogenic and anthropogenic contributions. Crustal dust dominates the elemental loadings across most sampling sites, particularly in the northern Antarctic Peninsula. While intercontinental transport (for example, ref. 39) cannot be ruled out, hundreds of square kilometres of ice-free areas serve as major sources of crustal dust in the northern Antarctic Peninsula. The observed decline in element concentrations associated with crustal dust towards southern latitudes probably reflects the reduced extent of ice-free areas and weaker wind transport.

Marine-enriched aerosols and biogenic sources play an important role in altering snow chemistry through nutrient cycling and the production of organic matter. In the Antarctic Peninsula, we found notable spatial variations in the concentrations of elements associated with biogenic activity (such as P), which are broadly consistent with previous studies reporting spatial patterns of algal blooms (for example, ref. 41). These findings suggest that algal proliferation is an important factor influencing the geochemical composition of Antarctic snow. The fact that 60% of algal blooms on the Antarctic Peninsula have been found within 5 km of a penguin colony[41] also indicates that algae are not the only biogenic source contributing to snow chemistry.

Concentrations of anthropogenic markers across our sampling sites significantly exceed background levels. Moderate EFs for heavy metals typically linked to fossil fuel pollution (Pb, Cu and Zn) were consistently found across all sampling sites, including Union Glacier (79° S), our southernmost sampling site. The highest concentrations were observed in northern sites, particularly around the South Shetland Islands, where dozens of research facilities are located and marine traffic is most intense.

Research activities in Antarctica are inherently energy intensive, involving the use of helicopters, watercraft, airplanes, diesel generators and all-terrain vehicles. The signature of these activities is now apparent in Antarctic snow chemistry, beyond heavily impacted sites near legacy research facilities. Much of the pollution associated with these facilities stems from wind redeposition of legacy pollutants but also from historically poor waste management practices. Although waste management has improved since the adoption of the Protocol on Environmental Protection, occasional waste incineration remains a potential source of heavy metal emissions. This may include Pb, especially when older materials containing lead-based paints or plastics and rubber with Pb-based stabilizers are burned.

Marine traffic in Antarctic waters has increased rapidly in recent years and is probably a growing source of pollution. Several countries have recently invested in new polar research vessels with icebreaking capabilities (for example, ref. 45). In addition, around a dozen fishing vessels regularly operate in Subarea 48.1, along the western side of the Antarctic Peninsula[46]. Still, tourism currently accounts for the majority of marine traffic in the region. IAATO now includes over 50 operators, with a fleet of 93 vessels (including 9 large cruise ships carrying more than 500 passengers) that collectively registered 569 departures during the 2023–2024 season[3].

The enrichment of heavy metals in Antarctic snow, even at sites kilometres away from local sources, stresses the large-scale extent of human activities. However, the concentrations of toxic elements commonly linked to fossil fuel pollution, such as As, Cd and Se, were found to be below the detection limit of the XRF spectrometry. Thus, beyond heavily impacted sites very close to research stations or legacy pollutants (for example, refs. 13–15), ecological impacts of heavy metals on Antarctic biota and microbial communities at current levels are unlikely to be widespread. Nonetheless, these impacts remain poorly understood and merit further investigation.

Our findings underscore the urgent need to advance sustainable practices to mitigate the footprint of human activities in Antarctica. In particular, the heavy metal traces found in our snow samples highlight the need for enhanced air pollution monitoring. Calls for enhanced environmental monitoring in the region date back to the 1990s (for

example, ref. 47). More recently, Brooks et al.[48] have outlined processes to help research station managers set objectives for reducing the impact of their facilities on nearby ecosystems. Tejedo et al.[49] have presented a strategy for monitoring environmental impacts of Antarctic tourism. Reducing the imprints of energy-intensive human activities in Antarctica will require accelerating the energy transition and minimizing the use of fossil fuels, especially near sensitive sites. The International Maritime Organization's ban on heavy fuel oil, the rapid adoption of hybrid vessels by the tourism industry and the voluntary implementation of a 40-km summertime buffer zone around the Antarctic Peninsula and the South Shetland Islands by krill harvesting companies[50] represent meaningful steps forward. Nevertheless, our results show that more remains to be done to reduce the burdens of human activities in Antarctica.

Methods

Sampling

A total of 55 surface snow samples (collected from depths of up to 15–20 cm, weighing approximately 2–3 kg each) were obtained using a methodology applied in previous studies (for example, ref. 6). As annual snowfall accumulation at all sampling sites far exceeds 15–20 cm, the snow we analysed originated from snowfall events that occurred in the preceding months. To ensure the representativeness of the sampled areas, sampling was carried out at distances, ranging from several hundred metres to several kilometres, from research infrastructure, tourist landing sites, roads, airfields, penguin colonies and wildlife nesting areas.

In an attempt to account for the expected variability in snow chemistry, we collected snow samples across multiple scales: (1) at distinct sites separated by tens to hundreds of kilometres, (2) at different sampling points within sites, spaced a few hundred metres apart, and (3) during different seasons at nearby locations. A detailed description of all sampling sites, including geographic coordinates and the season of collection, is provided in Table 1. As shown in the table, snow was sampled at 16 sites, some of which included multiple sampling points spaced several hundred metres apart. Duplicate samples (approximately 1 m apart) were also taken at each of the 28 sampling points listed (except for the one labelled 'Esperanza Station').

Sampling was primarily conducted in late summer. All sampling points were situated in close proximity (ranging from a few metres to several dozen metres) to ice-free areas. This ensured a consistent level of exposure to crustal and dust sources across the study sites. One exception was Ellsworth Mountains (79° S, 766 m a.s.l.), where sampling took place in early summer and the nearest crustal and dust sources are located several kilometres away. The focus on late summer sampling was intended to capture aerosols deposited on the snow surface during the annual peak in human activity in Antarctica. Snow that has persisted throughout the summer is expected to show the highest particulate concentrations of the season, as melting processes cause particles to accumulate on the surface[51].

To minimize contamination, strict protocols were followed. Tyvek clean suits and ultraclean medical gloves were worn during sampling, and samples were collected using precleaned stainless-steel spatulas. The collected snow was placed in plastic bags, which were then sealed in Whirlpak bags. Snow samples were transported to the laboratory in Styrofoam coolers. Upon arrival, the snow was melted in glass beakers and then vacuum-filtered to extract insoluble particles. Filtration was carried out using stainless-steel funnels and 0.4-µm Nucleopore filters, which were subsequently stored in sterile Petri dishes. During filtration, laboratory personnel wore gloves and laboratory coats, and all equipment and containers were rinsed with deionized water before use.

Chemical composition

Following a methodology applied in previous studies (for example, ref. 21), the elemental composition of particles deposited on filter medium was analysed using an Epsilon 5 EDXRF spectrometer (PANalytical). The Epsilon 5 system features a high-resolution germanium detector, enabling precise detection of elements from sodium to lead. The calibration procedure at HSPH, as described by Kang et al.[52], utilized XRF calibration standard polycarbonate films (MicroMatter). Intercomparison of standard films has demonstrated the high performance of the HSPH XRF spectrometer[52]. For field-collected samples (where elemental concentrations are generally lower), the instrument demonstrated reproducibility within 15% for the majority of elements analysed[52].

In this study, we found that the concentrations of 27 elements (out of the 48 targeted) exceeded the detection limits of the XRF spectrometry technique. These elements include Al, Si, P, S, Cl, K, Ca, Sc, Ti, V, Cr, Mn, Fe, Co, Ni, Cu, Zn, Ga, Br, Rb, Sr, Y, Zr, Ba and Pb (Supplementary Table 1). The concentrations of 21 elements (Ge, As, Se, Nb, Mo, Pd, Ag, Cd, In, Sn, Sb, Cs, La, Ce, Sm, Eu, Tb, W, Au, Hg and Tl) were generally under the detection limits. Therefore, these 21 elements were excluded from further analysis.

The concentrations measured in duplicate samples (taken approximately 1 m apart) remained within the same order of magnitude, supporting the reliability and consistency of our measurements. While differences in elemental concentrations were observed between sampling points separated by several hundred metres, or between samples collected in different seasons at nearby locations, these differences also generally remained within the same order of magnitude. Although relatively small, these variations were statistically significant (that is, they exceeded the estimated uncertainty bounds), probably reflecting real spatial variability in elemental abundance. Warren and Clarke[53] have reported significant spatial variability in particulate concentrations over horizontal distances of just a few metres in snow samples collected at the South Pole. They attributed this variability to the frequent occurrence of blizzards. While the snow redistribution processes observed at the South Pole may not be directly transferable to coastal environments on the Antarctic Peninsula, it is likely that blizzards also contribute to the observed differences in elemental concentrations between samples collected at the same site.

PCA

As shown in Supplementary Table 1, the differences in elemental concentrations observed between samples collected at different sites (taken dozens or hundreds of kilometres apart) were often substantial, sometimes exceeding an order of magnitude. Such variability provided valuable insights into potential sources of the measured elements.

PCA was performed on the concentrations in Supplementary Table 1 to reduce dimensionality and identify patterns in the dataset. The results are shown in Fig. 2, Supplementary Fig. 2 and Supplementary Tables 2–5. Before conducting PCA, the data underwent preprocessing to ensure comparability and minimize biases. This preprocessing included normalization and standardization. Log normalization was applied by calculating the natural logarithm (base e) of each data point to mitigate skewness and reduce the influence of extreme values. Subsequently, the data were standardized by subtracting the mean and dividing by the standard deviation for each variable, ensuring that all features contributed equally to the analysis, regardless of their original scales.

PCA results include the PC loadings and scores, presented in Supplementary Tables 2 and 3, respectively. The loadings indicate the contribution of each original variable to the PCs, while the scores represent the transformed data in the reduced-dimensional space. In addition, the percentage of variance explained by each PC is summarized in Supplementary Table 4. The first three PCs (PC1, PC2 and PC3) collectively accounted for 71% of the total variance in the concentrations in Supplementary Table 1. All computations were performed using Mathematica version 12[54].

Hierarchical clustering

We applied Ward's linkage as a criterion in the hierarchical clustering of our sampling sites. Ward's method is designed to minimize the

variance within clusters at each step of the hierarchical merging process. A dendrogram using Ward's linkage is shown in Supplementary Fig. 3. Computations were performed using Mathematica version 12[54].

Geochemical proxies

Elemental ratios derived from the measured concentrations were used as geochemical proxies to interpret geochemical processes and environmental conditions (for example, ref. 55). The following elemental ratios were calculated: Sr/Ca, Mg/Ca, P/Ca, Ti/Ca, Fe/Ca, Ti/Al, Zr/Al, Ba/Al, K/Al, Mg/Al, Mg/K, Si/K, Ca/K, Na/K, P/Al, Si/Al, Ca/Al, Sr/Ba, Ba/Si, K/Na, Ti/Zr, Si/Ti, P/Ti, Rb/Sr, K/Rb, Na/Mg, Ca/Mg, Ca/Sr, S/Na, Sr/Rb, K/Si and Fe/Al. These ratios were selected for their geochemical relevance, as they reflect mineralogical composition, diagenetic alterations and environmental changes, including redox conditions and biological productivity. For example, Ti/Al and Zr/Al ratios provide insights into terrigenous inputs (for example, ref. 56), while Mg/Al, Ca/Al and Fe/Al ratios have been used to distinguish different dust sources (for example, ref. 57). The calculated ratios are presented in Fig. 3b and Supplementary Table 6.

Enrichment factors

To evaluate the relative contributions of anthropogenic sources, we used crustal EF analysis as a diagnostic tool. The EF is defined as the ratio of the concentration of a given element to the concentration of the same element derived from crustal material (for example, rocks or dust). This approach distinguishes contributions of natural crustal sources from other potential inputs. According to the classifications outlined by Thamban and Thakur[34] and Veysseyre et al.[44], EF values in the range of 0.1–10 suggest minimal contributions from non-crustal sources, while values exceeding 10 indicate inputs from additional sources, which may include both natural and anthropogenic contributions. Specifically, EF values between 10 and 100 indicate moderate enrichment, while values greater than 100 suggest substantial enrichment from external sources.

For this analysis, we utilized upper continental crust composition data from Wedepohl[58], a widely recognized reference in geochemical studies. Following methodologies established in prior studies (for example, ref. 59), element concentrations were normalized against Al, a stable tracer for crustal material. EF values were calculated for each sampling site and are presented in Supplementary Table 7. Although some studies (for example, ref. 23) have normalized concentrations against Mn instead of Al, we found that, regardless of the normalization approach, EF values of key anthropogenic markers remained consistently high (Supplementary Table 8).

Marine traffic

Marine traffic data (Fig. 1a) comes from the IMF's World Seaborne Trade monitoring system[60], available at ref. 61.

Reanalysis

Surface wind speed (Supplementary Fig. 9), downwelling shortwave all-sky irradiance, and cloud fraction (CF) data (Supplementary Fig. 11) are derived from the ERA5 Atmospheric Reanalysis[62], available at ref. 63.

Back-trajectory analysis

Following prior efforts (for example, ref. 6), to trace the origin of air masses reaching selected sampling sites, we used the HYSPLIT model (Hybrid Single-Particle Lagrangian Integrated Trajectory)[64], driven by data from the Global Data Assimilation System, which provides outputs at a 1° spatial resolution and 3-h intervals[65]. For the selected sites, we computed 300-h backward trajectories for summer (December–January–February, DJF) days over the period 2014–2023. The 300-h (approximately 12.5 days) duration was chosen as it is sufficiently long to capture possible intercontinental aerosol transport (for example, ref. 26). The resulting trajectories were grouped into clusters using cluster analysis based on total spatial variance[66]. The results (Supplementary Fig. 12) support the premise of this study: local sources dominate aerosol emissions in our study area.

Ice-free areas

Geographically cross-referenced ice-free areas in Antarctica (Supplementary Fig. 4) come from Brooks[67].

Reporting summary

Further information on research design is available in the Nature Portfolio Reporting Summary linked to this article.

Data availability

The XRF spectrometry concentration data are available via Zenodo at https://doi.org/10.5281/zenodo.15823568 (ref. 68). Surface wind speed, downwelling shortwave all-sky irradiance and cloud fraction data are available at https://cds.climate.copernicus.eu/datasets/reanalysis-era5-single-levels-monthly-means?tab=download. Marine traffic data are available at https://datacatalog.worldbank.org/search/dataset/0037580/Global-Shipping-Traffic-Density. Geographically cross-referenced ice-free areas in Antarctica are available at https://data.aad.gov.au/metadata/AAS_5134_Antarctic_Disturbance_Footprint. Contact R.R.C. (raul.cordero@usach.cl) for inquiries and requests for materials. Source data are provided with this paper.

Code availability

The Mathematica code used in this study for the PCA is available via Zenodo at https://doi.org/10.5281/zenodo.15823599 (ref. 69).

References

1. Carrasco, J. F., Bozkurt, D. & Cordero, R. R. A review of the observed air temperature in the Antarctic Peninsula. Did the warming trend come back after the early 21st hiatus?. *Polar Sci.* **28**, 100653 (2021).
2. McCarthy, A. H., Peck, L. S. & Aldridge, D. C. Ship traffic connects Antarctica's fragile coasts to worldwide ecosystems. *Proc. Natl Acad. Sci. USA* **119**, e2110303118 (2022).
3. Overview of Antarctic vessel tourism: the 2023–24 season, and preliminary estimates for 2024–25. *IAATO* https://iaato.org/download/iaato-overview-of-antarctic-vessel-tourism-the-2023-24-season-and-preliminary-estimates-for-2024-25-atcm46_ip102_rev1_e_/ (2024).
4. *COMNAP Antarctic Facilities List* (Council of Managers of National Antarctic Programs, 2024); https://www.comnap.aq/s/Facilities_Nov2024.csv
5. Magalhães, N. et al. Seasonal changes in black carbon footprint on the Antarctic Peninsula due to rising shipborne tourism and forest fires. *Sci. Adv.* **10**, eadp1682 (2024).
6. Cordero, R. R. et al. Black carbon footprint of human presence in Antarctica. *Nat. Commun.* **13**, 984 (2022).
7. Khan, A. L., Klein, A. G., Katich, J. M. & Xian, P. Local emissions and regional wildfires influence refractory black carbon observations near Palmer Station, Antarctica. *Front. Earth Sci.* **7**, 49 (2019).
8. Khan, A. L. et al. Near-surface refractory black carbon observations in the atmosphere and snow in the McMurdo dry valleys, Antarctica, and potential impacts of Foehn winds. *J. Geophys. Res. Atmos.* **123**, 2877–2887 (2018).
9. Chen, L. C., Maciejczyk, P. & Thurston, G. D. in *Handbook on the Toxicology of Metals* (eds Nordberg, G. F. & Costa, M.) 137–182 (Academic Press, 2022).
10. Bargagli, R. & Rota, E. Environmental contamination and climate change in Antarctic ecosystems: an updated overview. *Environ. Sci. Adv.* **3**, 543–560 (2024).
11. Matias, R. S. et al. Mercury biomagnification in an Antarctic food web of the Antarctic Peninsula. *Environ. Pollut.* **304**, 119199 (2022).

12. Bargagli, R., Sanchez-Hernandez, J. C., Martella, L. & Monaci, F. Mercury, cadmium and lead accumulation in Antarctic mosses growing along nutrient and moisture gradients. *Polar Biol.* **19**, 316–322 (1998).
13. Stark, J. S. et al. Contamination of the marine environment by Antarctic research stations: monitoring marine pollution at Casey station from 1997 to 2015. *PLoS ONE* **18**, e0288485 (2023).
14. de Lima Neto, E. et al. Soil contamination by toxic metals near an Antarctic refuge in Robert Island, Maritime Antarctica: a monitoring strategy. *Water Air Soil Pollut.* **228**, 1–9 (2017).
15. Braga Bueno Guerra, M. et al. Heavy metals contamination in century-old manmade technosols of Hope Bay, Antarctic Peninsula. *Water Air Soil Pollut.* **222**, 91–102 (2011).
16. Chen, L. et al. Regional aerosol optical depth over Antarctica. *Atmos. Res.* **308**, 107534 (2024).
17. Fan, S., Gao, Y., Sherrell, R. M., Yu, S. & Bu, K. Concentrations, particle-size distributions, and dry deposition fluxes of aerosol trace elements over the Antarctic Peninsula in austral summer. *Atmos. Chem. Phys.* **21**, 2105–2124 (2021).
18. Bertler, N. et al. Snow chemistry across Antarctica. *Ann. Glaciol.* **41**, 167–179 (2005).
19. Kakareka, S., Kukharchyk, T. & Kurman, P. Trace and major elements in surface snow and fresh water bodies of the Marguerite Bay Islands, Antarctic Peninsula. *Polar Sci.* **32**, 100792 (2022).
20. Pizarro, J. et al. Contaminant emissions as indicators of chemical elements in the snow along a latitudinal gradient in southern Andes. *Sci. Rep.* **11**, 14530 (2021).
21. Alfonso, J. A. et al. Elemental and mineralogical composition of the Western Andean Snow (18°S–41°S). *Sci. Rep.* **9**, 8130 (2019).
22. Grigholm, B. et al. Chemical composition of fresh snow from Glaciar Marinelli, Tierra del Fuego, Chile. *J. Glaciol.* **55**, 769–776 (2009).
23. Gabrielli, P. et al. Variations in atmospheric trace elements in Dome C (East Antarctica) ice over the last two climatic cycles. *Atmos. Environ.* **39**, 6420–6429 (2005).
24. Bertinetti, S., Ardini, F., Vecchio, M. A., Caiazzo, L. & Grotti, M. Isotopic analysis of snow from Dome C indicates changes in the source of atmospheric lead over the last fifty years in East Antarctica. *Chemosphere* **255**, 126858 (2020).
25. Uetake, J. et al. Airborne bacteria confirm the pristine nature of the Southern Ocean boundary layer. *Proc. Natl Acad. Sci. USA* **117**, 13275–13282 (2020).
26. Asmi, E. et al. Primary sources control the variability of aerosol optical properties in the Antarctic Peninsula. *Tellus Ser. B* **70**, 1–16 (2018).
27. Tuohy, A. et al. Transport and deposition of heavy metals in the Ross Sea Region, Antarctica. *J. Geophys. Res. Atmos.* **120**, 10–996 (2015).
28. Wolff, E. W. & Peel, D. A. Closer to a true value for heavy metal concentrations in recent Antarctic snow by improved contamination control. *Ann. Glaciol.* **7**, 61–69 (1985).
29. Leal, M. A. et al. Atmospheric impacts due to anthropogenic activities in remote areas: the case study of Admiralty Bay/King George Island/Antarctic Peninsula. *Water Air Soil Pollut.* **188**, 67–80 (2008).
30. Hong, S. M., Lluberas, A., Lee, G. W. & Park, J. K. Natural and anthropogenic heavy metal deposition to the snow in King George Island, Antarctic Peninsula. *Ocean Polar Res.* **24**, 279–287 (2002).
31. Dixon, D. A. et al. Variations in snow and firn chemistry along US ITASE traverses and the effect of surface glazing. *Cryosphere* **7**, 515–535 (2013).
32. Grotti, M. et al. Year-round record of dissolved and particulate metals in surface snow at Dome Concordia (East Antarctica). *Chemosphere* **138**, 916–923 (2015).
33. Casey, K. A., Kaspari, S. D., Skiles, S. M., Kreutz, K. & Handley, M. J. The spectral and chemical measurement of pollutants on snow near South Pole, Antarctica. *J. Geophys. Res. Atmos.* **122**, 6592–6610 (2017).
34. Thamban, M. & Thakur, R. C. Trace metal concentrations of surface snow from Ingrid Christensen Coast, East Antarctica—spatial variability and possible anthropogenic contributions. *Environ. Monit. Assess.* **185**, 2961–2975 (2013).
35. Kakareka, S., Kukharchyk, T. & Kurman, P. Study of trace elements in the surface snow for impact monitoring in Vecherny Oasis, East Antarctica. *Environ. Monit. Assess.* **192**, 1–15 (2020).
36. Brooks, S. T., Jabour, J. & Bergstrom, D. M. What is 'footprint'in Antarctica: proposing a set of definitions. *Antarct. Sci.* **30**, 227–235 (2018).
37. da Silva, J. R. M. C., Bergami, E., Gomes, V. & Corsi, I. Occurrence and distribution of legacy and emerging pollutants including plastic debris in Antarctica: sources, distribution and impact on marine biodiversity. *Mar. Pollut. Bull.* **186**, 114353 (2023).
38. Kavan, J., Nývlt, D., Láska, K., Engel, Z. & Kňažková, M. High-latitude dust deposition in snow on the glaciers of James Ross Island, Antarctica. *Earth Surf. Proc. Land.* **45**, 1569–1578 (2020).
39. Gassó, S. & Torres, O. Temporal characterization of dust activity in the Central Patagonia desert (years 1964–2017). *J. Geophys. Res. Atmos.* **124**, 3417–3434 (2019).
40. Revell, L. E. et al. The sensitivity of Southern Ocean aerosols and cloud microphysics to sea spray and sulfate aerosol production in the HadGEM3-GA7.1 chemistry–climate model. *Atmos. Chem. Phys.* **19**, 15447–15466 (2019).
41. Gray, A. et al. Remote sensing reveals Antarctic green snow algae as important terrestrial carbon sink. *Nat. Commun.* **11**, 1–9 (2020).
42. Khan, A. L., Dierssen, H. M., Scambos, T. A., Höfer, J. & Cordero, R. R. Spectral characterization, radiative forcing and pigment content of coastal Antarctic snow algae: approaches to spectrally discriminate red and green communities and their impact on snowmelt. *Cryosphere* **15**, 133–148 (2021).
43. Jiang, X. et al. Spatial variations of Pb, As, and Cu in surface snow along the transect from the Zhongshan Station to Dome A, East Antarctica. *Sci. Cold Arid Reg.* **10**, 219–231 (2018).
44. Veysseyre, A. et al. Heavy metals in fresh snow collected at different altitudes in the Chamonix and Maurienne Valleys, French Alps: initial results. *Atmos. Environ.* **35**, 415–425 (2001).
45. Rogan-Finnemore, M. et al. Icebreaking polar class research vessels: new Antarctic fleet capabilities. *Polar Rec.* **57**, e46 (2021).
46. *Fishery Summary 2024: Euphausia superba in Area 48, CCAMLR Secretariat* (CCAMLR, 2025); https://fishdocs.ccamlr.org/FishSum_48_KRI_2024.pdf
47. Walton, D. W. & Shears, J. The need for environmental monitoring in Antarctica: baselines, environmental impact assessments, accidents and footprints. *Int. J. Environ. Anal. Chem.* **55**, 77–90 (1994).
48. Brooks, S. T. et al. Systematic conservation planning for Antarctic research stations. *J. Environ. Manag.* **351**, 119711 (2024).
49. Tejedo, P. et al. What are the real environmental impacts of Antarctic tourism? Unveiling their importance through a comprehensive meta-analysis. *J. Environ. Manag.* **308**, 114634 (2022).
50. *ARK Voluntary Measures* (Association of Responsible Krill Harvesting Companies, 2018); https://www.ark-krill.org/ark-vrz
51. Doherty, S. J. et al. Observed vertical redistribution of black carbon and other insoluble light-absorbing particles in melting snow. *J. Geophys. Res. Atmos.* **118**, 5553–5569 (2013).
52. Kang, C. M. et al. Interlab comparison of elemental analysis for low ambient urban $PM_{2.5}$ levels. *Environ. Sci. Technol.* **48**, 12150–12156 (2014).

53. Warren, S. G. & Clarke, A. D. Soot in the atmosphere and snow surface of Antarctica. *J. Geophys. Res. Atmos.* **95**, 1811–1816 (1990).
54. Mathematica Online (Wolfram Research, Inc., 2024).
55. Algeo, T. J. & Liu, J. A re-assessment of elemental proxies for paleoredox analysis. *Chem. Geol.* **540**, 119549 (2020).
56. Sun, Y., Wu, F., Clemens, S. C. & Oppo, D. W. Processes controlling the geochemical composition of the South China Sea sediments during the last climatic cycle. *Chem. Geol.* **257**, 240–246 (2008).
57. Gelado-Caballero, M. D. et al. Long-term aerosol measurements in Gran Canaria, Canary Islands: particle concentration, sources and elemental composition. *J. Geophys. Res. Atmos.* **117**, D03304 (2012).
58. Wedepohl, K. H. The composition of the continental crust. *Geoch. Cosm. Act.* **59**, 1217–1232 (1995).
59. Casalino, C. A., Malandrino, M., Giacomino, A. & Abollino, O. Total and fractionation metal contents obtained with sequential extraction procedures in a sediment core from Terra Nova Bay, West Antarctica. *Antar. Sci.* **25**, 83–98 (2013).
60. Cerdeiro, D. A., Komaromi, A., Liu, Y. & Saeed, M. *World Seaborne Trade in Real Time: A Proof of Concept for Building AIS-Based Nowcasts from Scratch (No. 20–57)* (International Monetary Fund, 2020).
61. Global shipping traffic density. *World Bank Group* https://datacatalog.worldbank.org/search/dataset/0037580/Global-Shipping-Traffic-Density (2023).
62. Hersbach, H. et al. ERA5 monthly averaged data on single levels from 1940 to present. *Copernicus Climate Change Service (C3S) Climate Data Store* https://doi.org/10.24381/cds.f17050d7 (2025).
63. ERA5 monthly averaged data on single levels from 1940 to present. *Climate Data Store* https://cds.climate.copernicus.eu/datasets/reanalysis-era5-single-levels-monthly-means?tab=download (2024).
64. Stein, A. F. et al. NOAA's HYSPLIT atmospheric transport and dispersion modeling system. *Bull. Am.* **96**, 2059–2077 (2015).
65. *Global Data Assimilation System (GDAS1) Archive Information* (NOAA Air Resources Laboratory, 2004); http://ready.arl.noaa.gov/gdas1.php
66. Su, L., Yuan, Z., Fung, J. C. & Lau, A. K. A comparison of HYSPLIT backward trajectories generated from two GDAS datasets. *Sci. Total Environ.* **506**, 527–537 (2015).
67. Brooks, S. T. *Our Footprint on Antarctica—Buildings, Disturbance* version 2 (Australian Antarctic Data Centre, 2019); https://doi.org/10.26179/5dc8db48eb58e
68. Cordero, R. R. XRF data. *Zenodo* https://doi.org/10.5281/zenodo.15823568 (2025).
69. Cordero, R. R. PCA code. *Zenodo* https://doi.org/10.5281/zenodo.15823599 (2025).
70. *Deep Field and Air Overview of Antarctic Tourism: 2023–24 Season and Preliminary Estimates for 2024–25 Season* (IAATO, 2024); https://iaato.org/system/files?file=2025-01/ATCM46_ip103_e_IAATO-Deep-Field-and-Air-Overview-of-Antarctic-Tourism-2023-24-Season-and-Preliminary-Estimates-for-2024-25-Season.pdf
71. Hunter, J. D. Matplotlib: a 2D graphics environment. *Comput. Sci. Eng.* **9**, 90–95 (2007).

Acknowledgements

The support of INACH (RT_69-20), ANID (ANILLO ACT210046, FONDECYT 1231904), USACH-DICYT 092431CC_Ayudante, NSF Award 2046240, and Antarctica XXI is gratefully acknowledged.

Author contributions

R.R.C., S.F., A.D., M.D., C.W., J.P., E.R., J.C., Z.O., P.O., M.L., A.B. and A.L.K wrote the paper. R.R.C., S.F., E.S., A.M. and F.F. analysed the data. E.S., J.A.A., B.G., J.M.C., P.L., P.W., J.J., J.D., G.C. and C.-M.K performed the experiments. All authors reviewed the paper.

Competing interests

The authors declare no competing interests.

Additional information

Supplementary information The online version contains supplementary material available at https://doi.org/10.1038/s41893-025-01616-7.

Correspondence and requests for materials should be addressed to Sarah Feron or Jaime Pizarro.

Peer review information *Nature Sustainability* thanks Andrew Klein and the other, anonymous, reviewer(s) for their contribution to the peer review of this work.

nature portfolio

Corresponding author(s): Feron, S.;Pizarro J., NATSUSTAIN-25021277A

Last updated by author(s): Jul 5, 2025

Reporting Summary

Nature Portfolio wishes to improve the reproducibility of the work that we publish. This form provides structure for consistency and transparency in reporting. For further information on Nature Portfolio policies, see our Editorial Policies and the Editorial Policy Checklist.

Statistics

For all statistical analyses, confirm that the following items are present in the figure legend, table legend, main text, or Methods section.

n/a	Confirmed	
☐	☒	The exact sample size (*n*) for each experimental group/condition, given as a discrete number and unit of measurement
☐	☒	A statement on whether measurements were taken from distinct samples or whether the same sample was measured repeatedly
☐	☒	The statistical test(s) used AND whether they are one- or two-sided *Only common tests should be described solely by name; describe more complex techniques in the Methods section.*
☒	☐	A description of all covariates tested
☐	☒	A description of any assumptions or corrections, such as tests of normality and adjustment for multiple comparisons
☐	☒	A full description of the statistical parameters including central tendency (e.g. means) or other basic estimates (e.g. regression coefficient) AND variation (e.g. standard deviation) or associated estimates of uncertainty (e.g. confidence intervals)
☐	☒	For null hypothesis testing, the test statistic (e.g. *F*, *t*, *r*) with confidence intervals, effect sizes, degrees of freedom and *P* value noted *Give P values as exact values whenever suitable.*
☒	☐	For Bayesian analysis, information on the choice of priors and Markov chain Monte Carlo settings
☒	☐	For hierarchical and complex designs, identification of the appropriate level for tests and full reporting of outcomes
☒	☐	Estimates of effect sizes (e.g. Cohen's *d*, Pearson's *r*), indicating how they were calculated

Our web collection on statistics for biologists contains articles on many of the points above.

Software and code

Policy information about availability of computer code

Data collection	No software was used for data collection.
Data analysis	Data analysis included the of Mathematica version 12

For manuscripts utilizing custom algorithms or software that are central to the research but not yet described in published literature, software must be made available to editors and reviewers. We strongly encourage code deposition in a community repository (e.g. GitHub). See the Nature Portfolio guidelines for submitting code & software for further information.

Data

Policy information about availability of data

All manuscripts must include a data availability statement. This statement should provide the following information, where applicable:

- Accession codes, unique identifiers, or web links for publicly available datasets
- A description of any restrictions on data availability
- For clinical datasets or third party data, please ensure that the statement adheres to our policy

The X-ray fluorescence (XRF) spectrometry concentrations are available at https://doi.org/10.5281/zenodo.15823568
Surface wind speed, downwelling shortwave (SW) all-sky irradiance, and cloud fraction (CF) data are available at https://cds.climate.copernicus.eu/datasets/reanalysis-era5-single-levels-monthly-means?tab=download
Marine traffic data are available at https://datacatalog.worldbank.org/search/dataset/0037580/Global-Shipping-Traffic-Density

Geographically cross-referenced ice-free areas in Antarctica are available at https://data.aad.gov.au/metadata/AAS_5134_Antarctic_Disturbance_Footprint
Contact the main author (raul.cordero@usach.cl) for inquiries and requests for materials.

Research involving human participants, their data, or biological material

Policy information about studies with human participants or human data. See also policy information about sex, gender (identity/presentation), and sexual orientation and race, ethnicity and racism.

Reporting on sex and gender	This study did not involve any human or biological material.
Reporting on race, ethnicity, or other socially relevant groupings	*Please specify the socially constructed or socially relevant categorization variable(s) used in your manuscript and explain why they were used. Please note that such variables should not be used as proxies for other socially constructed/relevant variables (for example, race or ethnicity should not be used as a proxy for socioeconomic status).* *Provide clear definitions of the relevant terms used, how they were provided (by the participants/respondents, the researchers, or third parties), and the method(s) used to classify people into the different categories (e.g. self-report, census or administrative data, social media data, etc.)* *Please provide details about how you controlled for confounding variables in your analyses.*
Population characteristics	*Describe the covariate-relevant population characteristics of the human research participants (e.g. age, genotypic information, past and current diagnosis and treatment categories). If you filled out the behavioural & social sciences study design questions and have nothing to add here, write "See above."*
Recruitment	*Describe how participants were recruited. Outline any potential self-selection bias or other biases that may be present and how these are likely to impact results.*
Ethics oversight	*Identify the organization(s) that approved the study protocol.*

Note that full information on the approval of the study protocol must also be provided in the manuscript.

Field-specific reporting

Please select the one below that is the best fit for your research. If you are not sure, read the appropriate sections before making your selection.

☐ Life sciences ☐ Behavioural & social sciences ☒ Ecological, evolutionary & environmental sciences

For a reference copy of the document with all sections, see nature.com/documents/nr-reporting-summary-flat.pdf

Ecological, evolutionary & environmental sciences study design

All studies must disclose on these points even when the disclosure is negative.

Study description	We analyze the chemistry of surface snow samples collected along a ~2,000 km transect, from the South Shetland Islands (62°S) to the Ellsworth Mountains (79°S) in Antarctica.
Research sample	A total of 55 surface snow samples (collected from depths of up to 15–20 cm, weighing approximately 2–3 kg each) were obtained.
Sampling strategy	In an attempt to account for the expected variability in snow chemistry, we collected snow samples across multiple scales: (i) at distinct sites separated by tens to hundreds of kilometers, (ii) at different sampling points within sites, spaced a few hundred meters apart, and (iii) during different seasons at nearby locations. A detailed description of all sampling sites, including geographic coordinates and the season of collection, is provided in Table 1. As shown in the table, snow was sampled at 16 sites, some of which included multiple sampling points spaced several hundred meters apart. Duplicate samples (approximately one meter apart) were also taken at each of the 28 sampling points listed (except for the one labeled "Esperanza Station").
Data collection	To minimize contamination, strict protocols were followed. Tyvek clean suits and ultraclean medical gloves were worn during sampling, and samples were collected using precleaned stainless-steel spatulas. The collected snow was placed in plastic bags, which were then sealed in Whirlpak bags. Snow samples were transported to the laboratory in Styrofoam coolers. Upon arrival, the snow was melted in glass beakers and then vacuum-filtered to extract insoluble particles. Filtration was carried out using stainless-steel funnels and 0.4-µm Nucleopore filters, which were subsequently stored in sterile petri dishes. During filtration, laboratory personnel wore gloves and lab coats, and all equipment and containers were rinsed with deionized water prior to use.
Timing and spatial scale	Sampling was primarily conducted in late summer. All sampling points were situated in close proximity (ranging from a few meters to several dozen meters) to ice-free areas. This ensured a consistent level of exposure to crustal and dust sources across the study sites. One exception was Ellsworth Mountains (79°S, 766 m a.s.l.), where sampling took place in early summer and the nearest crustal and dust sources are located several kilometers away. The focus on late summer sampling was intended to capture aerosols deposited on the snow surface during the annual peak in human activity in Antarctica.
Data exclusions	No data were excluded.
Reproducibility	Duplicate samples (approximately one meter apart) were also taken at each of the 28 sampling points listed (except for the one

Reproducibility	labeled "Esperanza Station").
Randomization	Randomization was not applied in this study as sampling locations were selected to capture spatial variability in aerosol deposition.
Blinding	Blinding was not implemented in this study, as the analyses were based on objective, instrument-based measurements (e.g. geochemical concentrations), and sample handling followed standardized protocols that minimize observer bias.

Did the study involve field work? ☒ Yes ☐ No

Field work, collection and transport

Field conditions	Sampling was primarily conducted in late summer. . The focus on late summer sampling was intended to capture aerosols deposited on the snow surface during the annual peak in human activity in Antarctica. Snow that has persisted throughout the summer is expected to show the highest particulate concentrations of the season, as melting processes cause particles to accumulate on the surface.
Location	The coordinates of each sampling site is indicated in Table 1
Access & import/export	Fieldwork was conducted with appropriate permissions (issued by the Chilean Antarctic Institute - INACH) and in accordance with local regulations and research ethics standards.
Disturbance	Since the samples were small and superficial, no relevant disturbance was caused.

Reporting for specific materials, systems and methods

We require information from authors about some types of materials, experimental systems and methods used in many studies. Here, indicate whether each material, system or method listed is relevant to your study. If you are not sure if a list item applies to your research, read the appropriate section before selecting a response.

Materials & experimental systems

n/a	Involved in the study
☒	☐ Antibodies
☒	☐ Eukaryotic cell lines
☒	☐ Palaeontology and archaeology
☒	☐ Animals and other organisms
☒	☐ Clinical data
☒	☐ Dual use research of concern
☒	☐ Plants

Methods

n/a	Involved in the study
☒	☐ ChIP-seq
☒	☐ Flow cytometry
☒	☐ MRI-based neuroimaging

Plants

Seed stocks	This study did not involve any plant or seed.
Novel plant genotypes	*Describe the methods by which all novel plant genotypes were produced. This includes those generated by transgenic approaches, gene editing, chemical/radiation-based mutagenesis and hybridization. For transgenic lines, describe the transformation method, the number of independent lines analyzed and the generation upon which experiments were performed. For gene-edited lines, describe the editor used, the endogenous sequence targeted for editing, the targeting guide RNA sequence (if applicable) and how the editor was applied.*
Authentication	*Describe any authentication procedures for each seed stock used or novel genotype generated. Describe any experiments used to assess the effect of a mutation and, where applicable, how potential secondary effects (e.g. second site T-DNA insertions, mosiacism, off-target gene editing) were examined.*